Phytopathology Research

RESEARCH

Open Access

The MAP4 kinase NbM4K3 regulates immune responses in *Nicotiana benthamiana*

Shuangxi Zhang[1], Haijuan Li[2], Meixiang Zhang[1*] and Yuyan An[1*]

Abstract

The mitogen-activated protein kinase kinase kinase kinase (M4K) family is evolutionarily conserved across plants and animals. In Arabidopsis, the protein kinase SIK1, an M4K member, is known to positively modulate reactive oxygen species (ROS) production during pattern-triggered immunity (PTI) by stabilizing BIK1, a key receptor-like cytoplasmic kinase (RLCK). While homologs of SIK1 exhibit conserved protein domain architectures across a range of land plants, their functional conservation remains incompletely understood. This study investigates the functional conservation and divergence of SIK1 homologs, focusing particularly on NbM4K3 in *Nicotiana benthamiana*. Silencing *NbM4K3* resulted in an impairment of the flg22-induced ROS burst and expression of PTI marker genes. Additionally, silencing *NbM4K3* led to diminished protein accumulation of RLCKs, while overexpression of the RLCKs prominently enhanced the flg22-induced ROS burst in *NbM4K3*-silenced plants. Furthermore, *NbM4K3*-silenced plants exhibited a compromised hypersensitive response (HR), reduced ROS accumulation, and diminished expression of effector-triggered immunity (ETI) marker genes when challenged with the avirulent strains *Ralstonia solanacearum* GMI1000 and *Pseudomonas syringae* DC3000, suggesting that NbM4K3 is a positive regulator of ETI. The attenuated HR phenotype observed in *NbM4K3*-silenced plants upon expression of RipP1 or RipE1, two avirulent type III effectors of GMI1000, further supports the affirmative role of NbM4K3 in ETI. In summary, our data indicate that the M4K NbM4K3 positively regulates both PTI and ETI in *N. benthamiana*, potentially by stabilizing RLCKs. These findings not only strengthen the role of M4K family in plant immunity but also suggest its potential in improving disease resistance in plants.

Keywords NbM4K3, ROS burst, Pattern-triggered immunity, Effector-triggered immunity, RLCK

Background

In response to continual threats posed by pathogens, plants have evolved a sophisticated immune system to combat pathogen infections, comprising pattern-triggered immunity (PTI) and effector-triggered immunity (ETI) (Chisholm et al. 2006; Jones and Dangl 2006). Upon pathogen invasion, plants employ pattern-recognition receptors (PRRs) on the cell membranes to initiate a cascade of signaling pathways (Zipfel 2014; Tang et al. 2017), including calcium influx, generation of reactive oxygen species (ROS), activation of protein kinases, and transcriptional reprogramming (Couto and Zipfel 2016; Wang et al. 2020). These coordinated responses form the backbone of PTI. However, pathogens often deploy effectors to subvert PTI, prompting plants to evolve intracellular nucleotide-binding site and leucine-rich repeat domain receptors (NLRs) that initiates ETI (Chisholm et al. 2006; Cui et al. 2015). ETI typified by a hypersensitive response (HR) effectively confines pathogen growth at the infection site (Monteiro et al. 2018).

*Correspondence:
Meixiang Zhang
meixiangzhang@snnu.edu.cn
Yuyan An
anyuyan@snnu.edu.cn
[1] College of Life Sciences, National Engineering Laboratory for Endangered Medicinal Resource Development in Northwest China/Key Laboratory of Medicinal Resources and Natural Pharmaceutical Chemistry of Ministry of Education, Shaanxi Normal University, Xi'an 710119, China
[2] College of Biological and Environmental Engineering, Xi'an University, Xi'an 710065, China

The extracellular ROS burst plays a vital role in both PTI and ETI in plants (Yuan et al. 2021a). During PTI, ROS burst reinforces the cell wall and triggers downstream responses upon recognition of pathogen-associated molecular patterns (PAMPs) by PRRs (Kadota et al. 2014). This process involves the activation of the receptor-like cytoplasmic kinase BIK1, which phosphorylates respiratory burst oxidase homolog D (RBOHD), thereby promoting ROS production (Kadota et al. 2014; Li et al. 2014). In addition to BIK1, other PTI-associated protein kinases, such as PBLs, CPKs, SIK1, and CRK2, also contribute to RBOHD phosphorylation and subsequent extracellular ROS production in Arabidopsis(Kadota et al. 2014; Li et al. 2014; Zhang et al. 2018; Kimura et al. 2020). NLRs, upon detecting specific effectors, not only initiate ETI but also enhance the levels of key immune proteins like BIK1 and RBOHD, which are involved in ETI-induced cell death (Kadota et al. 2019). The increased levels of these immune proteins amplify ROS generation and the expression of key immune genes, thereby reinforcing the plant's defense mechanisms (Yuan et al. 2021b; Yu et al. 2024). Despite these insights, the regulation of ROS burst in other plant species is not fully understood.

The mitogen-activated protein kinase kinase kinase kinase (M4K) family is evolutionarily conserved in both plants and animals. Its role in human immunity has been well-documented (Brenner et al. 2009; Jiao et al. 2015; Zhang et al. 2018). It is conceivable that M4K proteins are also involved in plant immunity. Indeed, SIK1 (AtM4K3), an Arabidopsis M4K, has been identified as a positive regulator of plant immunity, which promotes ROS burst during PTI by stabilizing BIK1 and activating RBOHD activity (Xiong et al. 2016; Zhang et al. 2018). BIK1 and RBOHD are also implicated in ROS production during ETI, apart from their involvement in PTI (Yuan et al. 2021b). However, whether M4K participates in ETI responses remains unknown. Additionally, *sik1* mutants exhibited enhanced resistance alongside autoimmune responses, suggesting a delicate balance in plant immunity (Zhang et al. 2018). Similar domain architectures are observed in SIK1 homologs across various land plants (Zhang et al. 2018), raising the question of whether the homologs, such as NbM4K3 in *Nicotiana benthamiana*, share similar immune functions. Unraveling the functional mechanisms of these homologs could provide a broader understanding of plant immune regulation.

In this study, we focus on NbM4K3, a member of the M4K family in *N. benthamiana*, and investigate its roles in PTI and ETI responses. By silencing *NbM4K3*, we observed a reduced ROS burst triggered by flg22, and the plant did not exhibit autoimmunity. We further explored the mechanism by which NbM4K3 regulates ROS burst during PTI. Importantly, we also uncovered the positive role of NbM4K3 in regulating ETI and the involvement of receptor-like cytoplasmic kinases (RLCKs) in NbM4K3-regulated ROS burst during both PTI and ETI. Our findings provide insights into the functional mechanism of M4K3 in bridging PTI and ETI interactions.

Results

NbM4K3 positively regulates flg22-induced ROS production

Previous research has elucidated the involvement of SIK1 (AtM4K3) in flg22-triggered ROS burst in Arabidopsis (Zhang et al. 2018). However, the potential contribution of NbM4K3, a homolog of SIK1, to flg22-induced ROS burst remains uncertain. In this study, we identified two M4K3 homologs, NbM4K3a and NbM4K3b, in *N. benthamiana* (Fig. 1a and Additional file 1: Figure S1). Since NbM4K3a and NbM4K3b share a high degree of nucleotide sequence similarity, we utilized a 300-bp DNA fragment to silence both *NbM4K3a* and *NbM4K3b* to generate *NbM4K3*-silenced plants (TRV: *NbM4K3*). Notably, TRV: *NbM4K3 N. benthamiana* plants exhibited significant growth inhibition, characterized by small and wrinkled leaves, and alterations in leaf morphology (Fig. 1b), suggesting a similar function of NbM4K3 to SIK1 in cell proliferation and expansion (Xiong et al. 2016). RT-qPCR analysis confirmed the silencing of *NbM4K3*, evidenced by a significant decrease of its transcription level (Fig. 1c). Subsequently, we compared the flg22-induced ROS burst in TRV: *NbM4K3* plants with that in TRV: *GFP* control plants. Strikingly, *NbM4K3* silencing caused a significant decrease (about 50%) in flg22-induced ROS burst (Fig. 1d, e), aligning with findings observed in *sik1* mutants (Zhang et al. 2018). In addition, the ROS burst induced by chitin was also impaired in *NbM4K3*-silenced plants (Additional file 1: Figure S2). In *sik1* mutants, the PAMP-induced mitogen-activated protein kinase (MAPK) activation is not impaired (Zhang et al. 2018). Here, upon exposure to flg22, the MAPK activation was also not impaired in *NbM4K3*-silenced plants (Additional file 1: Figure S3). Together, these results imply a conserved role of M4K3 in PAMP-induced ROS production and MAPK activation.

Silencing of *NbM4K3* impairs plant immunity

The *sik1* mutants display autoimmunity, activated salicylic acid (SA) signaling pathway, and enhanced resistance against *Pseudomonas syringae* DC3000 in Arabidopsis (Zhang et al. 2018). In this study, we investigated the impact of *NbM4K3* silencing on *N. benthamiana* resistance to the oomycete pathogen *Phytophthora parasitica*. Results showed that the lesion size of *P. parasitica* in leaves of *NbM4K3*-silenced plants increased by

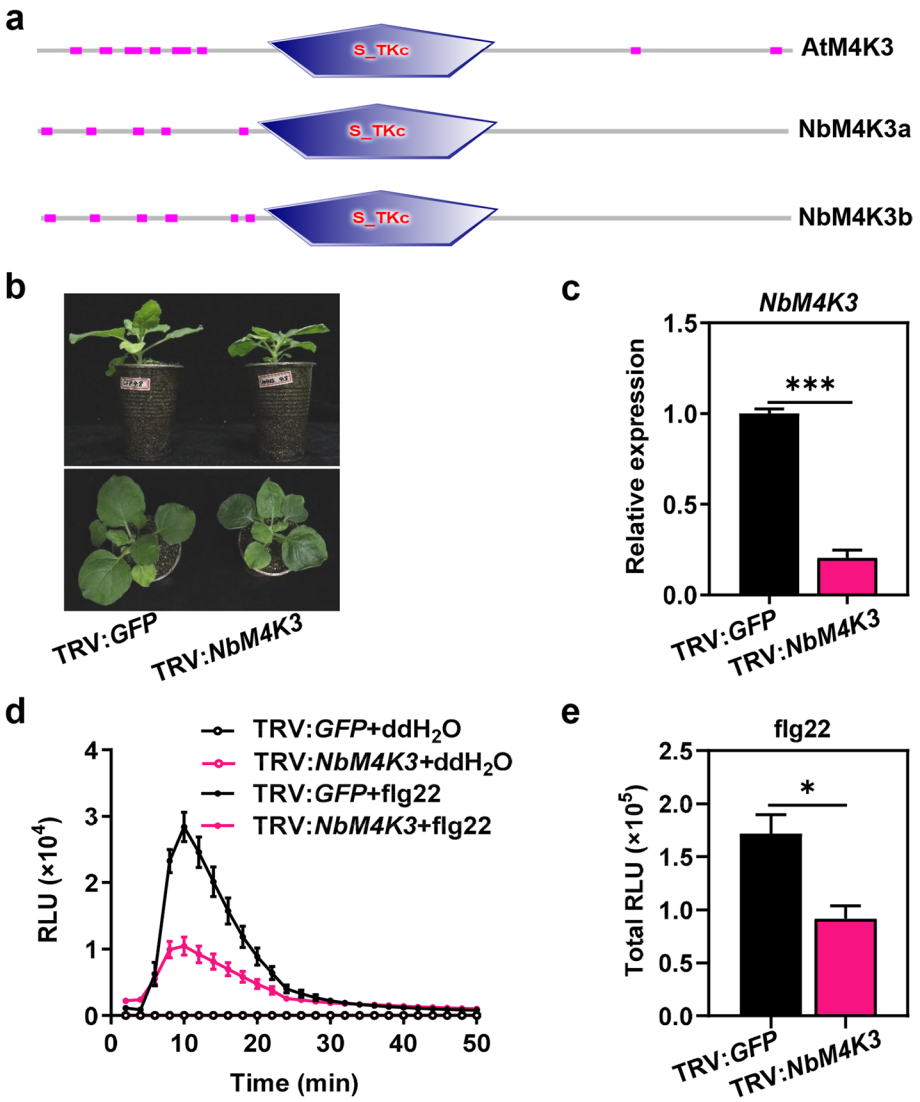

Fig. 1 Involvement of NbM4K3 in flg22-induced ROS burst in *Nicotiana benthamiana*. **a** The protein domain of AtM4K3, NbM4K3a, and NbM4K3b predicted by SMART. S_TKc stands for Serine/Threonine protein kinases, catalytic domain. **b** Phenotype of 4-week-old *NbM4K3*-silenced plants. **c** *NbM4K3* expression analysis in **b** by RT-qPCR. **d** The curve of ROS burst in *NbM4K3*-silenced and *GFP*-silenced plants after treatment with 100 nM flg22. **e** Total ROS accumulation in **d**. Data are shown as mean ± SE (n=12). Experiments were repeated three times with similar results. The statistical analysis was performed using Student's t-test, with * $p < 0.05$ and *** $p < 0.001$ indicating significance

20% compared to *GFP*-silenced plants (Fig. 2a, b), indicating the compromised disease resistance in *NbM4K3*-silenced plants. To confirm this observation, we further compared bacterial growth in *NbM4K3*-silenced and *GFP*-silenced plants upon infection with the virulent strain *P. syringae* DC3000 Δ*hopQ1-1*, which lacks the type III effector HopQ1 (Schultink et al. 2017). Similar to the response observed upon *P. parasitica* infection, colonization of DC3000 Δ*hopQ1-1* in leaves of *NbM4K3*-silenced plants was higher than that in the control (Fig. 2c), confirming that *NbM4K3* silencing diminishes plant immunity. Additionally, the expression level of *PR1a*, a marker gene for SA signaling (Dean et al. 2005), in *NbM4K3*-silenced plants was comparable to that in the control plants (Fig. 2d), suggesting that unlike SIK1, silencing of *NbM4K3* does not induce autoimmunity.

NbM4K3-silenced plants exhibit decreased expression of PTI-related genes upon flg22 induction

The above results showed that the ROS burst and disease resistance were compromised in *NbM4K3*-silenced plants. To elucidate the impact of *NbM4K3* silencing on PTI, we examined the expression of PTI marker genes, *ACRE31*, *CYP71D20*, and *PTI5* (Heese et al. 2007; Zhong

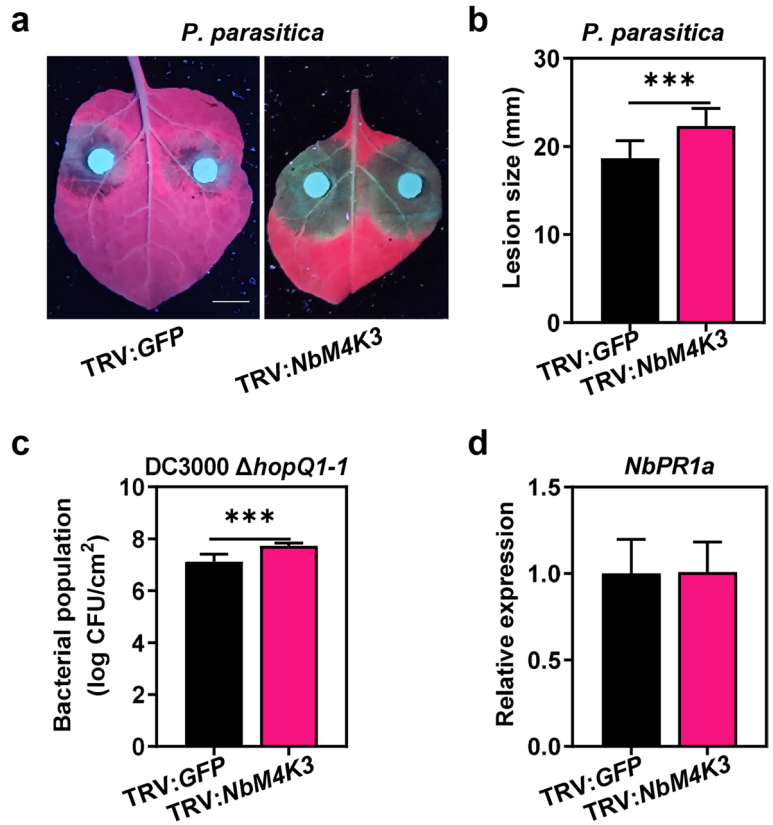

Fig. 2 Reduced plant basal defense in *NbM4K3*-silenced *N. benthamiana*. **a** Phenotype of *P. parasitica*-inoculated leaves of *NbM4K3*- or *GFP*-silenced plants at 2 days post-inoculation (dpi) under UV light. Scale bars: 10 mm. **b** Quantification of the lesion diameters in **a**. Data are shown as mean ± SD (*n*=12). **c** The bacterial population at 3 dpi in *NbM4K3*-silenced plants that were leaf-inoculated with *P. syringae* DC3000 Δ*hopQ1-1*. Data are shown as mean ± SD (*n*=6). **d** The expression levels of *NbPR1a* in 4-week-old *N. benthamiana* leaves. Experiments were repeated three times with similar results. The statistical analysis was performed using Student's *t*-test, with *** $p < 0.001$ indicating significance

et al. 2018). The results showed that silencing of *NbM4K3* resulted in significant downregulation of *CYP71D20* and *PTI5* transcription (Fig. 3). After treatment with flg22 for 1 h, the expression levels of all three PTI marker genes in *NbM4K3*-silenced plants were significantly decreased compared to those in *GFP*-silenced plants (Fig. 3). The decreased expression of PTI marker genes in *NbM4K3*-silenced plants indicated that NbM4K3 positively regulates PTI, and importantly, no autoimmunity was observed in *NbM4K3*-silenced plants.

Accumulation of BIK1 homologous RLCKs was reduced in *NbM4K3*-silenced plants

The RLCK BIK1 plays a crucial role in the innate defense response of plants and ROS generation (Yuan et al. 2021a; Liu and Tang 2023). SIK1 positively regulates PTI by interacting with and stabilizing BIK1 (Zhang et al. 2018). Given the conservation of NbM4K3 and SIK1 in PTI regulation, we hypothesized that NbM4K3 may also function through modulating homologs of BIK1 in *N. benthamiana*. We identified four BIK1 homologous RLCKs in *N. benthamiana*, which share the same domain as BIK1 (Fig. 4a and Additional file 1: Figure S4). Luciferase complementation assays (LCA) showed that NbM4K3b interacted with these BIK1 homologs in *N. benthamiana* (Additional file 1: Figure S5). Remarkably, the abundance of these BIK1 homologs was significantly reduced in *NbM4K3*-silenced plants compared to the control, while the accumulation of NbCRK42, a homolog of AtCRK42, remained unchanged (Fig. 4b and Additional file 1: Figure S6). These findings suggest that *NbM4K3* silencing leads to instability of the BIK1 homologous RLCKs.

Over-expression of BIK1 homologous RLCKs enhances flg22-induced ROS burst in *NbM4K3*-silenced *N. benthamiana*

To investigate the role of BIK1 homologous RLCKs in NbM4K3-mediated ROS burst during PTI responses,

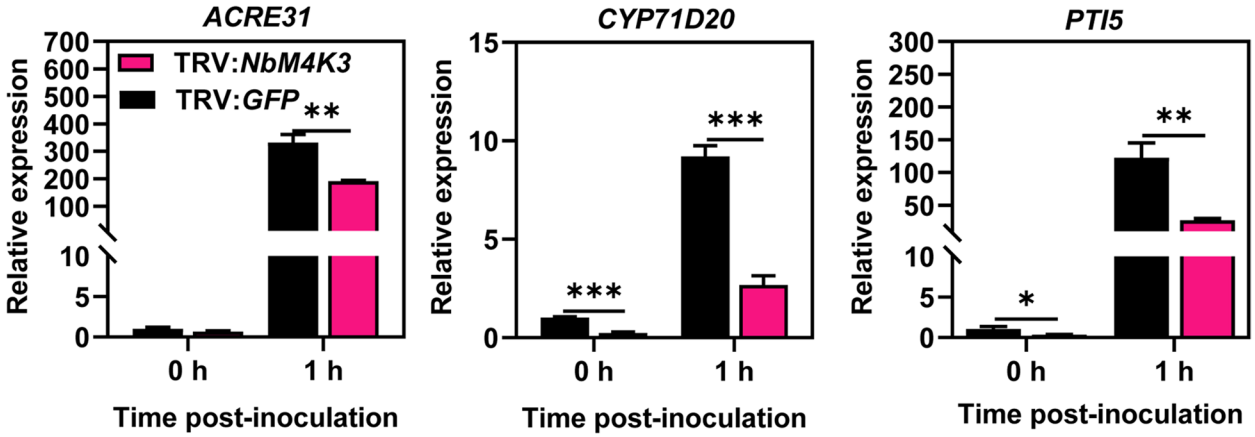

Fig. 3 Reduced expression levels of PTI marker genes in *NbM4K3*-silenced plants upon flg22 treatment. The relative expression levels of PTI marker genes, *ACRE31*, *CYP71D20*, and *PTI5*, in 5-week-old *NbM4K3*-silenced plants. Leaves were treated with 1 μM flg22 for 1 h, and gene expression at 0 h and 1 h were measured by RT-qPCR. Experiments were repeated three times with similar results. The statistical analysis was performed using Student's *t*-test, with ** $p < 0.01$ and *** $p < 0.001$ indicating significance

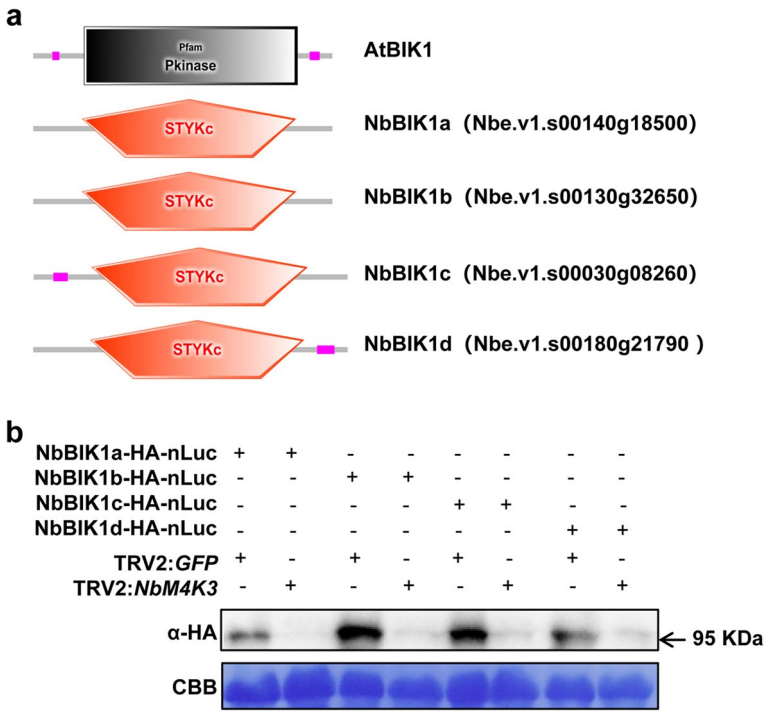

Fig. 4 Decreased protein accumulation of BIK1 homologous RLCKs in *NbM4K3*-silenced *N. benthamiana*. **a** The protein domains of AtBIK1 and NbBIK1 predicted by SMART. Both Pkinase and STYKc stand for protein kinase domain. **b** The protein abundance of NbBIK1s in 5-week-old *NbM4K3*- and *GFP*-silenced plants. NbBIK1-HA-nluc was expressed in 5-week-old *N. benthamiana* leaves. Samples were collected at 48 h after infiltration. NbBIK1 was detected by an anti-HA antibody. Experiments were repeated three times with similar results

we individually overexpressed these RLCKs in *NbM4K3*-silenced *N. benthamiana* and examined their effects on flg22-induced ROS burst. LTI6b, a protein unrelated to plant immunity, was used as the negative control (Martinière et al. 2011; Lee et al. 2020). Compared with LTI6b, the expression of three BIK1 homologs significantly enhanced flg22-induced ROS burst in *NbM4K3*-silenced plants, whereas NbBIK1d did not (Fig. 5), suggesting that NbBIK1d may not contribute to NbM4K3-mediated ROS burst. Additionally, protein expression of NbBIK1d was

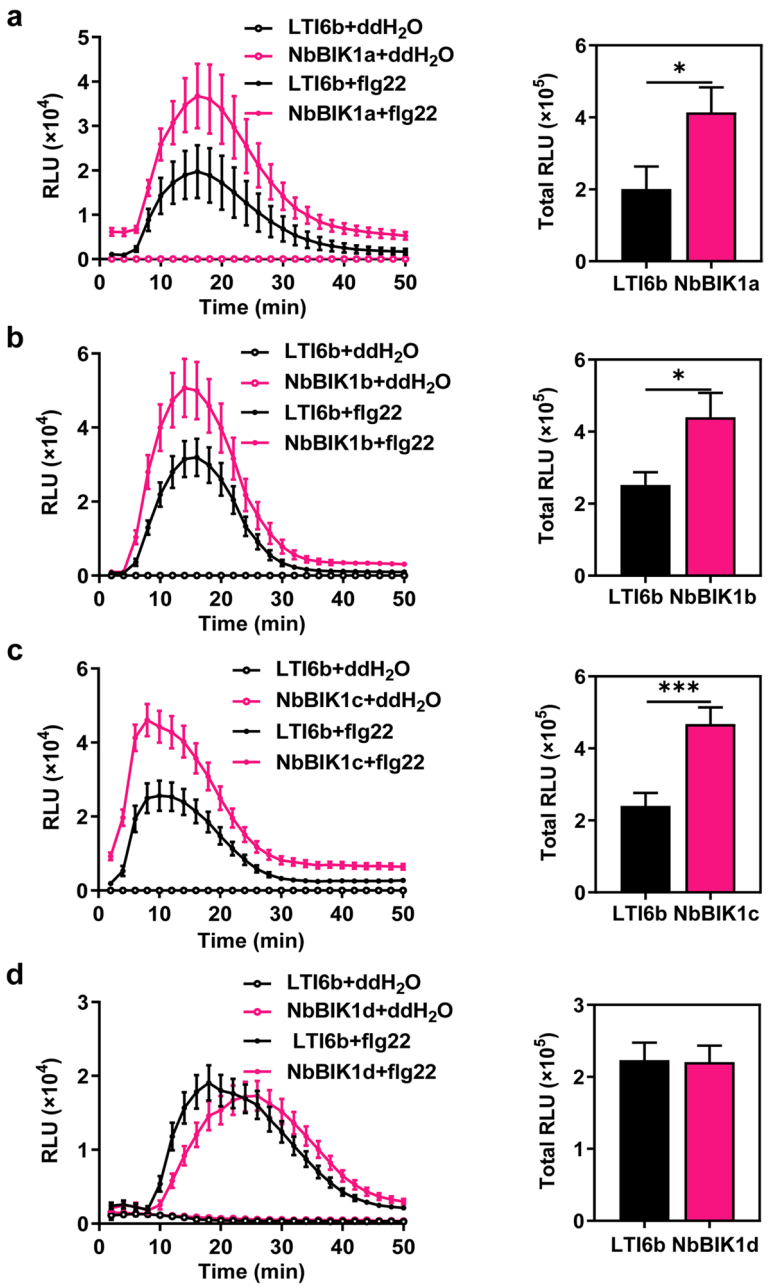

Fig. 5 Enhanced flg22-induced ROS burst in *NbM4K3*-silenced plants by expressing of BIK1 homologous RLCKs. **a**–**d** The effect of transiently expressed NbBIK1a, NbBIK1b, NbBIK1c, and NbBIK1d on flg22-induced ROS burst in *NbM4K3*-silenced plants. LTI6b was used as a negative control. GV3101 cells containing NbBIK1 or LTI6b with an OD_{600} of 0.4 were infiltrated into the leaves of *NbM4K3*-silenced plants. Then the leaves were used for 100 nM flg22-induced ROS burst assays 48 h after agroinfiltration. Data of total ROS accumulation are shown as mean ± SE (n=12). Experiments were repeated three times with similar results. The statistical analysis was performed using Student's t-test, with * $p < 0.05$ and *** $p < 0.001$ indicating significance

confirmed in the silenced plants by western blot (Additional file 1: Figure S7). These results imply that similar to SIK1, NbM4K3 regulates PTI by enhancing the stability of RLCKs in *N. benthamiana*.

NbM4K3 regulates ETI

Recent studies have highlighted the involvement of BIK1 and RBOHD in ROS burst during ETI (Ngou et al. 2021; Yuan et al. 2021b). Given that SIK1 and NbM4K3 positively regulate ROS burst by stabilizing BIK1 or its

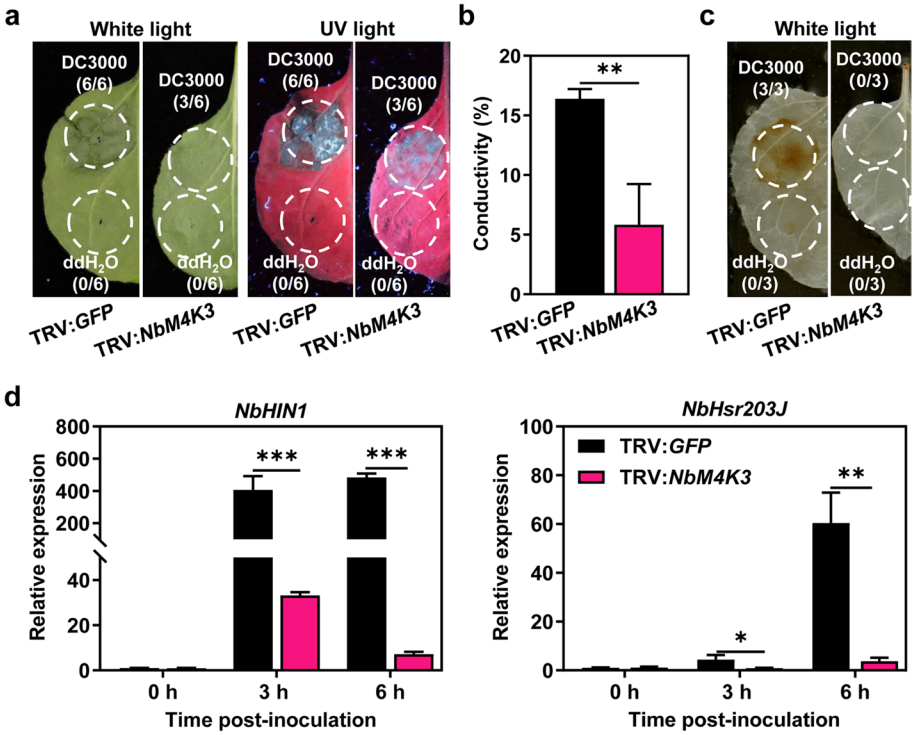

Fig. 6 NbM4K3 positively regulates ETI induced by *P. syringae* DC3000. **a** Phenotype of HR induced by inoculation of DC3000 (OD_{600}=0.001) at 3 dpi. **b** Cell death was evaluated by the degree of ion leakage. The degree of ion leakage from the leaf discs was measured 2 days after infiltration using a conductivity meter. Data are mean ± SD (*n*=3). **c** H_2O_2 accumulation at 1 dpi by DAB staining in **a**. **d** Expression levels of *NbHIN1* and *NbHsr203J* induced by DC3000 (OD_{600}=0.001). Experiments were repeated three times with similar results. Data are means ± SD (*n*=12). The statistical analysis was performed using Student's *t*-test, with * $p < 0.05$, ** $p < 0.01$, and *** $p < 0.001$ indicating significance

homologs in plants, we propose that M4K3 may also be involved in ETI. *Ralstonia solanacearum* GMI1000 and *P. syringae* DC3000 can be recognized in *N. benthamiana* (Thomas et al. 2020) and induce typical HR (Poueymiro et al. 2009; Liu et al. 2013). We injected DC3000 and GMI1000 into TRV: *GFP* and TRV: *NbM4K3* plants, respectively, and observed the HR phenotypes at three days post-inoculation (dpi) to investigate the role of M4K3 in ETI.

Compared to the *GFP*-silenced plants, DC3000-induced HR was noticeably weaker in *NbM4K3*-silenced plants (Fig. 6a). The significantly lower ion leakage in *NbM4K3*-silenced plants supports the reduced HR in plants (Fig. 6b). We further assessed the effect of *NbM4K3* silencing on hydrogen peroxide (H_2O_2) production during ETI using the DAB staining method (Scharte et al. 2005). Results showed that DC3000-triggered H_2O_2 accumulation in *NbM4K3*-silenced plants was significantly lower than that in control plants (Fig. 6c). Furthermore, the expression levels of ETI-related genes, *NbHIN1* and *NbHsr203J* (Kumar et al. 2015), were monitored. We observed a significant decrease in both *NbHIN1* and *NbHsr203J* expression at 3 and 6 hours post-DC3000 inoculation in *NbM4K3*-silenced plants compared to control plants (Fig. 6d). These results collectively demonstrate an impaired ETI response to DC3000 in *NbM4K3*-silenced plants.

To confirm the role of NbM4K3 in ETI responses, we investigated the effect of *NbM4K3* knockdown on HR induced by GMI1000. Similarly, significant reductions were found in HR phenotype (Fig. 7a), ion leakage (Fig. 7b), H_2O_2 accumulation (Fig. 7c), and expression of ETI marker genes (Fig. 7d) in *NbM4K3*-silenced plants. Additionally, silencing of *NbM4K3* significantly impaired the cell death phenotype induced by two avirulent type III effectors of GMI1000, RipP1 and RipE1 (Landry et al. 2020) (Fig. 7e). These findings provide direct evidence that NbM4K3 not only participates in PTI responses but also positively regulates ETI responses in plants.

Discussion

Plants resist pathogen invasion through a two-layered innate immune system, PRRs-mediated PTI, and NLRs-mediated ETI (Jones and Dangl 2006). Both PTI and ETI have been extensively studied over the past three decades. It is well-established that PTI and ETI share numerous

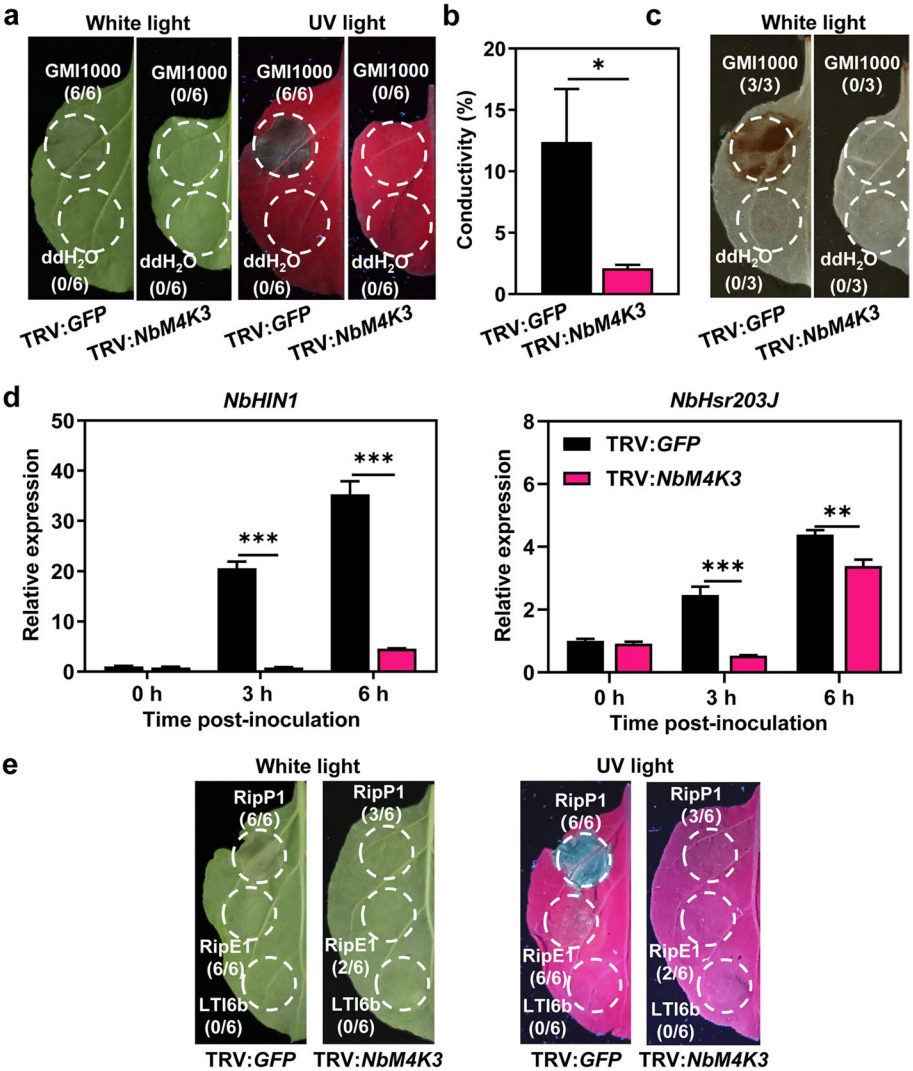

Fig. 7 NbM4K3 positively regulates ETI induced by *R. solanacearum* GMI1000. **a** Phenotype of HR induced by GMI1000 (OD_{600}=0.05) at 3 dpi. **b** Cell death is evaluated by the degree of ion leakage. The degree of ion leakage from the leaf discs was measured 2 days after infiltration using a conductivity meter. Data are means ± SD (n=3). **c** H_2O_2 accumulation at 1 dpi by DAB staining in **a**. **d** Expression levels of *NbHIN1* and *NbHsr203J* induced by GMI1000. Data are mean ± SD (n=3). **e** HR induced by avirulent effectors RipP1 and RipE1 at 3 dpi. LTI6b was used as a negative control. GV3101 cells containing pER8-effector or LTI6b with an OD_{600} of 0.4 were infiltrated into the leaves. The estradiol was applied to the leaves 24 h after agroinfiltration. The leaves were photographed at 3 d after estradiol treatment. Circles indicate the infiltrated area. The fraction represents the number of HR over the total number of the infiltrated leaves. Experiments were repeated three times with similar results. The statistical analysis was performed using Student's t-test, with ** $p < 0.01$ and *** $p < 0.001$ indicating significance

similar responses, such as ROS burst and MAPK activation. The intricate interplay between PTI and ETI is crucial for achieving effective plant disease resistance (Ngou et al. 2022). However, the precise mechanisms underlying their interaction remain elusive. The M4K protein family, known for its evolutionary conservation, has been implicated in human immune systems (Brenner et al. 2009; Jiao et al. 2015; Zhang et al. 2018). Previous research has unveiled the positive involvement of the M4K SIK1 in PTI in Arabidopsis (Zhang et al. 2018). In this study, we demonstrate that a M4K member, NbM4K3, positively regulates not only PTI but also ETI in *N. benthamiana*, suggesting NbM4K3 as a crucial candidate that orchestrates the mutual potentiation between PTI and ETI.

In Arabidopsis, SIK1 acts as a positive regulator of PTI by enhancing BIK1 stability to promote PAMP-induced ROS burst (Zhang et al. 2018). In this study, we found that NbM4K3 shares a similar domain architecture with SIK1, and its knockdown resulted in significant suppression of flg22-induced ROS burst in *N. benthamiana*

(Fig. 1), similar to the findings in *sik1* (Zhang et al. 2018). Concurrently with the generation of ROS, PTI also triggers the activation of MAPKs (Couto and Zipfel 2016). However, in *sik1* mutant, the PAMP-induced MAPK activation is not impaired (Zhang et al. 2018). Here, a similar result was obtained in *NbM4K3*-silenced plants, indicating that M4K3 primarily regulates PAMP-induced ROS production.

Additionally, the expression of PTI marker genes, *ACRE31*, *CYP71D20*, and *PTI5* (Heese et al. 2007; Zhong et al. 2018), was markedly compromised upon *NbM4K3* silencing in response to flg22 treatment (Fig. 3). These results underscore the conserved function of M4K3 in modulating ROS burst during PTI in plants.

BIK1, a member of the RLCK family, plays a crucial role in SIK1-mediated ROS burst and PTI (Zhang et al. 2018). BIK1 has emerged as a key regulator of ROS accumulation in plants (Kadota et al. 2019; Ngou et al. 2021; Yuan et al. 2021b). In this study, NbM4K3 interacts with BIK1 homologs in *N. benthamiana,* and *NbM4K3* knockdown caused the instability of these BIK1 homologs (Fig. 4 and Additional file 1: Figure S5). Furthermore, the expression of 3 out of 4 BIK1 homologous RLCKs significantly promoted ROS burst upon flg22 treatment in *NbM4K3*-silenced plants (Fig. 5). These findings suggest that NbM4K3 facilitates ROS burst during PTI by stabilizing BIK1 homologous RLCKs. The stability of BIK1 is known to mainly rely on the phosphorylation of S236 (Wang et al. 2018; Zhang et al. 2018), a site conserved among BIK1 homologs (Additional file 1: Figure S4). Therefore, it is plausible that NbM4K3 can phosphorylate BIK1 homologous RLCKs at S236 to stabilize these proteins.

In *sik1* mutant, there is a notable accumulation of SA, leading to the activation of the SA signaling pathway (Zhang et al. 2018). Consequently, *sik1* mutant displays increased resistance against *P. syringae*, indicating the triggering of an autoimmune response (Zhang et al. 2018). In contrast, our study observed a substantial decrease in resistance of *NbM4K3*-silenced plants to *P. parasitica* and DC3000 Δ*hopQ1-1*, implying that silencing *NbM4K3* does not induce an autoimmune response. It is important to note, however, that we cannot rule out the possibility that the observed non-autoimmune phenotype could be attributed to residual expression levels of *NbM4K3* (Fig. 1). Additionally, we did not observe a significant alteration in the expression of *PR1a*, a SA marker gene (Dean et al. 2005), in *NbM4K3*-silenced plants (Fig. 2). These findings underscore the functional distinctions between NbM4K3 and its Arabidopsis homolog SIK1, despite their conservation in regulating PTI. Similar studies about the functional discrepancy between homologs of important immune proteins have been reported. For instance, the autoimmune phenotype present in the maize G protein beta subunit mutant was not observed in the *Arabidopsis* homologs (Wu et al. 2020). It is worth uncovering the mechanisms underlying such differences. In Arabidopsis, it is conceivable that an evolutionary mechanism, such as the presence of a NLR, has emerged to monitor SIK1. Mutations in SIK1 may be perceived by the plant, subsequently triggering autoimmunity. However, this regulatory system may not be present in *N. benthamiana*, as the SIK1 homolog NbM4K3 may not be subjected to similar regulation mechanisms. Further research is needed to fully understand the functional discrepancies among M4K3 homologs across different plant species and to elucidate the mechanisms that account for these differences.

ROS generation plays pivotal roles not only in PTI but also in ETI. The RLCK BIK1 has been identified as a critical regulator of ROS accumulation in both PTI and ETI responses (Kadota et al. 2019; Ngou et al. 2021; Yuan et al. 2021b; Yu et al. 2024). SIK1 and NbM4K3 regulate the stability of BIK1 in Arabidopsis and its homologous RLCKs in *N. benthamiana*. It is reasonable to speculate that M4K3 may also positively regulate ETI. *R. solanacearum* GMI1000 and *P. syringae* DC3000 can induce ETI in *N. benthamiana* (Thomas et al. 2020). In this study, silencing *NbM4K3* significantly impaired GMI1000- and DC3000-induced HR, validating our hypothesis of M4K3's involvement in ETI (Figs. 6 and 7). The HR phenotypes induced by the expression of RipP1 and RipE1, two avirulent effectors in GMI1000, were also suppressed in *NbM4K3*-silenced plants. Moreover, the expression of ETI-related genes was significantly downregulated in *NbM4K3*-silenced plants during GMI1000- and DC3000-induced ETI. These results confirm the positive role of NbM4K3 in ETI. Furthermore, ROS production during GMI1000- and DC3000-induced ETI was also significantly decreased (Figs. 6 and 7). These findings demonstrate that NbM4K3 is involved in not only PTI but also ETI. Considering the enhancement of the stability of BIK1 homologous RLCKs by NbM4K3 and the pivotal role of these RLCKs on ROS regulation, it is plausible to conclude that NbM4K3 positively regulates both PTI and ETI through manipulation of RLCK stability. In light of the pivotal role that NbM4K3 plays in both PTI and ETI, our findings underscore the potential of this protein and its homologs as targets for enhancing disease resistance in plant breeding programs.

Conclusions

In summary, our study highlights the significant contribution of NbM4K3 in plant immunity in *N. benthamiana*, impacting both PTI and ETI. NbM4K3 facilitates ROS burst during both PTI and ETI by stabilizing

RLCKs. These findings shed lights on the role of the M4K family in plant immunity, and position it as a crucial mediator in the crosstalk between PTI and ETI. This finding prompts further exploration into the precise molecular mechanisms underlying its functions in future research endeavors.

Methods

Plant materials and bacterial strains

N. benthamiana plants were grown at 24°C under a long-day (16 h light/ 8 h dark) photoperiod. *Agrobacterium tumefaciens* strain GV3101 and *Escherichia coli* strain DH5α were cultured on Luria-Bertani (LB) agar plates or in LB liquid medium supplemented with appropriate antibiotics at 28°C and 37°C, respectively. *R. solanacearum* strain GMI1000 was cultivated at 28°C using Bacto-agar and Glucose (BG) medium. *P. syringae* DC3000 *ΔhopQ1-1* and DC3000 were grown in modified Luria-Bertani liquid medium (LM) at 28°C. *P. parasitica* was cultured at 28°C in V8 Juice Broth medium.

Vector construction

The coding sequences of *NbM4K3a*, *NbM4K3b*, or *NbBIK1* were amplified from *N. benthamiana* cDNA. The DNA fragments of *NbM4K3a* and *NbM4K3b* were cloned into pCambia1300-cCLuc, respectively. The DNA fragments of *NbBIK1a*, *NbBIK1b*, *NbBIK1c*, or *NbBIK1d* were cloned into the vector pCambia1300-HA-nCLuc, respectively. All sequences were confirmed by Sanger sequencing. Primers used were listed in Additional file 2: Table S1.

Bacterial inoculation assay

The bacterial inoculation assays for *P. syringae* strain DC3000 Δ*hopQ1-1* were performed according to the previously described method (Ouyang et al. 2023).

Phytophthora inoculations

The mycelial plugs were transferred from the original *P. parasitica* culture plate onto fresh V8 agar medium and placed in a constant temperature incubator set at 28°C for 3–4 days. An inoculation tray was prepared with three layers of filter paper saturated with 80 mL of sterile water. Inoculation involved using at least six leaves from 4-week-old plants, with each leaf having a 2 cm-long petiole wrapped in moistened cotton and positioned on the tray. Mycelial plugs of *Phytophthora* were then placed on the underside of the leaf, and 18 μL of sterile water was added to ensure complete contact between the plug and the leaf surface. The inoculation tray was sealed, covered with plastic, and incubated in a constant temperature incubator at 22°C for 36–60 hours in darkness. Leaf lesions were examined at 2 dpi using a handheld ultraviolet lamp, and the size of each lesion was quantified using ImageJ software (http://rsb.info.nih.gov/ij).

Virus-induced gene silencing

A 300-bp DNA fragment shared between *NbM4K3a* and *NbM4K3b* was cloned into the pTRV2 vector to silence both genes simultaneously. A combination of the pTRV2-GFP and pTRV1 vector was used as a control. Two-week-old *N. benthamiana* seedlings were utilized for gene silencing, and the gene-silenced plants were subjected to assays two weeks later. Gene-specific primers (Additional file 2: Table S1) were used for amplification purposes.

ROS burst assay

The flg22- and chitin-induced ROS burst were carried out according to a previously described method (Zhang et al. 2018; Li et al. 2022). ROS burst was analyzed by quantifying the accumulation of ROS triggered by 100 nM flg22 or 0.01% chitin over 30 minutes using luminescence measured with a multimode reader. The luminescence signals were detected for 500 ms per well, and the data were analyzed and presented based on the kinetics of ROS production, reported as relative luminescence units (RLU).

Luciferase complementation assay (LCA)

LCA was performed as previously described (Cao et al. 2022).

DAB staining

DAB staining was performed following a previously described protocol (Scharte et al. 2005). Leaves were immersed in 50 mL DAB solution (1 mg/mL DAB, pH3.8) with 25 μL Tween 20 (0.05% v/v), and 2.5 mL 200 mM Na_2HPO_4. Subsequently, the leaves were subjected to vacuum infiltration for 10 min to ensure thorough uptake of the DAB solution. Finally, the leaves were immersed in boiling ethanol (96%, v/v) for 10 min. A dark-brown spot indicates the reaction of DAB with H_2O_2.

Hypersensitive response (HR) assay

The HR assay was conducted following a previously described method with a slight modification (Zhang et al. 2024). *A. tumefaciens* GV3101 cells containing pER8-effectors were adjusted to an OD_{600} of 0.4 and the cells were infiltrated into tobacco leaves using a needleless syringe. Subsequently, 50 μM estradiol was applied to the leaves 24 hours after infiltration. Photographs of the leaves were taken 4 days after estradiol treatment.

For DC3000, bacterial suspensions were adjusted to OD_{600} of 0.001 and infiltrated into tobacco leaves using a needleless syringe. Similarly, for GMI1000, bacterial

suspensions were adjusted to OD_{600} of 0.05 and infiltrated into tobacco leaves using a needleless syringe. Three days after infiltration, the leaves were photographed.

Western blot

Proteins extracted from *N. benthamiana* leaves were separated via SDS-PAGE and transferred onto PVDF membranes obtained from Thermo Fisher. The PVDF membranes were then blocked using a solution of 5% defatted milk in TBST buffer (1× TBS with 0.05% Tween 20) for 60 minutes at room temperature. Subsequently, the membranes were incubated with anti-HA (1:10,000; Abmart, China), anti-flag (1:10,000; Abmart, China), or anti-phospho-p44/42 MAPKs (1:1000; Cell Signaling Technologies, USA) at room temperature for 1 h, respectively, followed by treatment with a horseradish peroxidase-conjugated secondary antibody (1:10,000; Sigma, China) for an additional 45 minutes. The resulting signals were visualized and captured using the SuperSignal West Pico Chemiluminescent substrate (Thermo Scientific, USA) with the Bio-Rad ChemiDoc Touch Imaging System (Bio-Rad, USA).

RT-qPCR analysis

Total RNA was isolated utilizing the Total RNA Extraction Kit following the manufacturer's instructions from Sangon Biotech (Shanghai, China). Subsequently, the RNA samples were reverse transcribed in a 20 μL reaction using the ABScript II cDNA First-Strand Synthesis Kit from ABclonal Technology (ABclonal, China). PCR analysis was conducted using SYBR Green to evaluate the relative expression levels of genes associated with defense and growth, with *NbEF1α* serving as the internal control. Changes in gene transcript levels were quantified utilizing the $2^{-\Delta\Delta Ct}$ method. The primer sequences for RT-qPCR can be found in Additional file 2: Table S1.

Statistical analysis

Each experiment was performed with a minimum of three biological duplicates. Duncan's multiple range tests were used with a significance level set at $p < 0.05$. Intergroup comparisons were statistically evaluated through Student's *t*-test, with significance levels denoted as * $p < 0.05$, ** $p < 0.01$, and *** $p < 0.001$.

Abbreviations

ETI	Effector-triggered immunity
HR	Hypersensitive response
M4K	Mitogen-activated protein kinase kinase kinase kinase
NLRs	Nucleotide-binding site and leucine-rich repeat domain receptors
PAMPs	Pathogen-associated molecular patterns
PTI	Pattern-triggered immunity
PPRs	Pattern-recognition receptors
RBOHD	Respiratory burst oxidase homolog D
RLCK	Receptor-like cytoplasmic kinase
ROS	Reactive oxygen species

Supplementary Information

The online version contains supplementary material available at https://doi.org/10.1186/s42483-024-00265-6.

Additional file 1: Figure S1. Conservation of the M4K3 kinase domain. **Figure S2.** The curve of chitin-induced ROS burst and total ROS accumulation in *NbM4K3*-silenced and *GFP*-silenced plants. **Figure S3.** MAPK activation was detected after flg22 treatment. **Figure S4.** Conservation of BIK1. **Figure S5.** NbM4K3 interacted with NbBIK1. **Figure S6.** The protein abundance of NbCRK42-FLAG in 5-week-old *NbM4K3*-silenced and *GFP*-silenced plants. **Figure S7.** The protein levels of NbBIK1d of Fig. 5d.

Additional file 2: Table S1. Primers used in this study.

Acknowledgments

Not applicable.

Authors' contributions

MZ and YA conceived and designed the experiments. SZ and HL carried out the experiments. All authors analyzed the data. SZ, MZ, and YA wrote the manuscript. All authors read and approved the final manuscript.

Funding

This work was supported by the National Natural Science Foundation of China (32072399, 32302296, 32372483), the Technology Innovation Leading Program of Shaanxi (2023QYPY2-01), the Fundamental Research Funds for the Central Universities (GK202201017, GK202207024), and the Natural Science Basic Research Program of Shaanxi (2024JC-YBMS-143).

Availability of data and materials

The datasets used and/or analyzed during the current study are available from the corresponding author upon reasonable request.

Declarations

Ethics approval and consent to participate

Not applicable.

Consent for publication

Not applicable.

Competing interests

The authors declare that they have no competing interests.

Received: 6 April 2024 Accepted: 12 June 2024
Published online: 30 August 2024

References

Brenner D, Brechmann M, Röhling S, Tapernoux M, Mock T, Winter D, et al. Phosphorylation of CARMA1 by HPK1 is critical for NF-κB activation in T cells. Proc Natl Acad Sci USA. 2009;106:14508–13. https://doi.org/10.1073/pnas.0900457106.

Cao P, Chen J, Wang R, Zhao M, Zhang S, An Y, et al. A conserved type III effector RipB is recognized in tobacco and contributes to *Ralstonia solanacearum* virulence in susceptible host plants. Biochem Bioph Res Co. 2022;631:18–24. https://doi.org/10.1016/j.bbrc.2022.09.062.

Chisholm ST, Coaker G, Day B, Staskawicz BJ. Host-microbe interactions: shaping the evolution of the plant immune response. Cell. 2006;124:803–14. https://doi.org/10.1016/j.cell.2006.02.008.

Couto D, Zipfel C. Regulation of pattern recognition receptor signaling in plants. Nat Rev Immunol. 2016;16:537–52. https://doi.org/10.1038/nri.2016.77.

Cui H, Tsuda K, Parker JE. Effector-triggered immunity: from pathogen perception to robust defense. Annu Rev Plant Biol. 2015;66:487–511. https://doi.org/10.1146/annurev-arplant-050213-040012.

Dean J, Goodwin P, Hsiang T. Induction of glutathione S-transferase genes of *Nicotiana benthamiana* following infection by *Colletotrichum destructivum* and *C. orbiculare* and involvement of one in resistance. J Exp Bot. 2005;56:1525–33. https://doi.org/10.1093/jxb/eri145.

Heese A, Hann DR, Gimenez-Ibanez S, Jones AM, He K, Li J, et al. The receptor-like kinase SERK3/BAK1 is a central regulator of innate immunity in plants. Proc Natl Acad Sci USA. 2007;104:12217–22. https://doi.org/10.1073/pnas.0705306104.

Jiao S, Zhang Z, Li C, Huang M, Shi Z, Wang Y, et al. The kinase MST4 limits inflammatory responses through direct phosphorylation of the adaptor TRAF6. Nat Immunol. 2015;16:246–57. https://doi.org/10.1038/ni.3097.

Jones JD, Dangl JL. The plant immune system. Nature. 2006;444:323–9. https://doi.org/10.1038/nature05286.

Kadota Y, Sklenar J, Derbyshire P, Stransfeld L, Asai S, Ntoukakis V, et al. Direct regulation of the NADPH oxidase RBOHD by the PRR-associated kinase BIK1 during plant immunity. Mol Cell. 2014;54:43–55. https://doi.org/10.1016/j.molcel.2014.02.021.

Kadota Y, Liebrand TW, Goto Y, Sklenar J, Derbyshire P, Menke FL, et al. Quantitative phosphoproteomic analysis reveals common regulatory mechanisms between effector-and PAMP-triggered immunity in plants. New Phytol. 2019;221:2160–75. https://doi.org/10.1111/nph.15523.

Kimura S, Hunter K, Vaahtera L, Tran HC, Citterico M, Vaattovaara A, et al. CRK2 and C-terminal phosphorylation of NADPH oxidase RBOHD regulate reactive oxygen species production in Arabidopsis. Plant Cell. 2020;32:1063–80. https://doi.org/10.1105/tpc.19.00525.

Kumar D, Kirti PB. Pathogen-induced SGT1 of *Arachis diogoi* induces cell death and enhanced disease resistance in tobacco and peanut. Plant Biotechnol J. 2015;13:73–84. https://doi.org/10.1111/pbi.12237.

Landry D, Gonzalez-Fuente M, Deslandes L, Peeters N. The large, diverse, and robust arsenal of *Ralstonia solanacearum* type III effectors and their in planta functions. Mol Plant Pathol. 2020;21:1377–88. https://doi.org/10.1111/mpp.12977.

Lee D, Lal NK, Lin ZD, Ma S, Liu J, Castro B, et al. Regulation of reactive oxygen species during plant immunity through phosphorylation and ubiquitination of RBOHD. Nat Commun. 2020;11:1838. https://doi.org/10.1038/s41467-020-15601-5.

Li L, Li M, Yu L, Zhou Z, Liang X, Liu Z, et al. The FLS2-associated kinase BIK1 directly phosphorylates the NADPH oxidase RbohD to control plant immunity. Cell Host Microbe. 2014;15:329–38. https://doi.org/10.1016/j.chom.2014.02.009.

Li Y, Zhang Q, Gong L, Kong J, Wang X, Xu G, et al. Extra-large G proteins regulate disease resistance by directly coupling to immune receptors in *Nicotiana benthamiana*. Phytopathol Res. 2022;4:49. https://doi.org/10.1186/s42483-022-00155-9.

Liu J, Tang D. Plant immunity research in China. Phytopathol Res. 2023;5:37. https://doi.org/10.1186/s42483-023-00196-8.

Liu Y, Wang L, Cai G, Jiang S, Sun L, Li D. Response of tobacco to the *Pseudomonas syringae* pv. *tomato* DC3000 is mainly dependent on salicylic acid signaling pathway. FEMS Microbiol Lett. 2013;344:77–85. https://doi.org/10.1111/1574-6968.12157.

Martinière A, Shvedunova M, Thomson AJ, Evans NH, Penfield S, Runions J, et al. Homeostasis of plasma membrane viscosity in fluctuating temperatures. New Phytol. 2011;192:328–37. https://doi.org/10.1111/j.1469-8137.2011.03821.x.

Monteiro F, Nishimura MT. Structural, functional, and genomic diversity of plant NLR proteins: an evolved resource for rational engineering of plant immunity. Annu Rev Phytopathol. 2018;56:243–67. https://doi.org/10.1146/annurev-phyto-080417-045817.

Ngou BPM, Ahn HK, Ding PT, Jones JDG. Mutual potentiation of plant immunity by cell-surface and intracellular receptors. Nature. 2021;592:110–5. https://doi.org/10.1038/s41586-021-03315-7.

Ngou BPM, Ding PT, Jones JDG. Thirty years of resistance: Zig-zag through the plant immune system. Plant Cell. 2022;34:1447–78. https://doi.org/10.1093/plcell/koac041.

Ouyang X, Chen J, Sun Z, Wang R, Wu X, Li B, et al. Ubiquitin E3 ligase activity of *Ralstonia solanacearum* effector RipAW is not essential for induction of plant defense in *Nicotiana benthamiana*. Front Microbiol. 2023;14:1201444. https://doi.org/10.3389/fmicb.2023.1201444.

Poueymiro M, Cunnac S, Barberis P, Deslandes L, Peeters N, et al. Two type III secretion system effectors from *Ralstonia solanacearum* GMI1000 determine host-range specificity on tobacco. Mol Plant Microbe In. 2009;22:538–50. https://doi.org/10.1094/Mpmi-22-5-0538.

Scharte J, Schön H, Weis E. Photosynthesis and carbohydrate metabolism in tobacco leaves during an incompatible interaction with *Phytophthora nicotianae*. Plant Cell Environ. 2005;28:1421–35. https://doi.org/10.1111/j.1365-3040.2005.01380.x.

Schultink A, Qi T, Lee A, Steinbrenner AD, Staskawicz B. Roq1 mediates recognition of the Xanthomonas and Pseudomonas effector proteins XopQ and HopQ1. Plant J. 2017;92:787–95. https://doi.org/10.1111/tpj.13715.

Tang D, Wang G, Zhou JM. Receptor kinases in plant-pathogen interactions: more than pattern recognition. Plant Cell. 2017;29:618–37. https://doi.org/10.1105/tpc.16.00891.

Thomas NC, Hendrich CG, Gill US, Allen C, Hutton SF, Schultink A. The immune receptor Roq1 confers resistance to the bacterial pathogens *Xanthomonas*, *Pseudomonas syringae*, and *Ralstonia* in tomato. Front Plant Sci. 2020;11:463. https://doi.org/10.3389/fpls.2020.00463.

Wang J, Grubb LE, Wang J, Liang X, Li L, Gao C, et al. A regulatory module controlling homeostasis of a plant immune kinase. Mol Cell. 2018;69:493–504. https://doi.org/10.1016/j.molcel.2017.12.026.

Wang W, Feng B, Zhou JM, Tang D. Plant immune signaling: Advancing on two frontiers. J Integr Plant Biol. 2020;62:2–24. https://doi.org/10.1111/jipb.12898.

Wu Q, Xu F, Liu L, Char SN, Ding Y, Je BI, et al. The maize heterotrimeric G protein β subunit controls shoot meristem development and immune responses. Proc Natl Acad Sci USA. 2020;117:1799–805. https://doi.org/10.1073/pnas.1917577116.

Xiong J, Cui X, Yuan X, Yu X, Sun J, Gong Q. The Hippo/STE20 homolog SIK1 interacts with MOB1 to regulate cell proliferation and cell expansion in Arabidopsis. J Exp Bot. 2016;67:1461–75. https://doi.org/10.1093/jxb/erv538.

Yu XQ, Niu HQ, Liu C, Wang HL, Yin W, Xia X. PTI-ETI synergistic signal mechanisms in plant immunity. Plant Biotechnol J. 2024. https://doi.org/10.1111/pbi.14332.

Yuan M, Ngou BPM, Ding PT, Xin XF. PTI-ETI crosstalk: an integrative view of plant immunity. Curr Opin Plant Biol. 2021;62(2021a):102030. https://doi.org/10.1016/j.pbi.2021.102030.

Yuan M, Jiang Z, Bi G, Nomura K, Liu M, Wang Y, et al. Pattern-recognition receptors are required for NLR-mediated plant immunity. Nature. 2021b;592:105–9. https://doi.org/10.1038/s41586-021-03316-6.

Zhang M, Chiang YH, Toruño TY, Lee D, Ma M, Liang X, et al. The MAP4 kinase SIK1 ensures robust extracellular ROS burst and antibacterial immunity in plants. Cell Host Microbe. 2018;24:379–91. https://doi.org/10.1016/j.chom.2018.08.007.

Zhang S, Cao P, Xiao Z, Zhang Q, Qiang Y, Meng H, et al. *Rastonia solanacearum* type III effectors target host 14–3-3 proteins to suppress plant immunity. Biochem Bioph Res Co. 2024;690:149256. https://doi.org/10.1016/j.bbrc.2023.149256.

Zhong C, Ren Y, Qi Y, Yu X, Wu X, Tian Z. PAMP-responsive ATL gene *StRFP1* and its orthologue *NbATL60* positively regulate *Phytophthora infestans* resistance in potato and *Nicotiana benthamiana*. Plant Sci. 2018;270:47–57. https://doi.org/10.1016/j.plantsci.2018.01.016.

Zipfel C. Plant pattern-recognition receptors. Trends Immunol. 2014;35:345–51. https://doi.org/10.1016/j.it.2014.05.004.